Iranian Journal of Chemistry and Chemical Engineering (IJCCE)

Enhancing Chemical and Mechanical Stability of Knee Prostheses in Orthopedic Applications: Development of Ceramic Nanoparticle-Reinforced Carbon Nanocomposites for Sports-Related Use

Rui Zhang[1], Jinyuan Zhuo[2]*

[1]College of science, North China University of Technology, Beijing, China, 100144

[2]PE Department, Renmin University of China, Beijing, China, 100084

Corresponding author: zhuojinyuan@ruc.edu.cn

Abstract

The incorporation of nanoparticles into composites has attracted significant attention from researchers due to their ability to enhance mechanical and physical properties without adding excessive weight. Nanoceramics, a type of nanoparticle, possess unique geometric and chemical characteristics and have widespread applications across various industries. In this study, the researchers investigated the influence of nanoceramics on the mechanical behavior of hybrid epoxy/glass fiber composites under ballistic loading conditions. The hybrid samples were fabricated using an innovative vacuum-assisted resin transfer molding technique (VARTM) and were subjected to tension and flexure tests. The results demonstrated that the hybrid samples exhibited improved mechanical properties compared to the control sample. Among the samples, the 3% nanoceramics sample demonstrated the most favorable performance, exhibiting increased elastic modulus, ultimate tensile strength, and flexural strength compared to the pure sample. Ballistic impact tests revealed that the ballistic efficiency initially decreased with increasing nanoceramics content but eventually increased when the concentration reached 7%. The ballistic limit velocities and the absorbed energy by the target varied depending on the nanoceramics content. These findings highlight the strain rate sensitivity of glass fibers and the potential of nanoceramics to enhance the ballistic properties of composites.

Keywords: *CNT Composites, Nanoceramic platelets, Hybrid materials, Sport application, Ballistic impact, Mechanical properties*

1. Introduction

In recent years, the properties of lightweight and high-strength polymeric composite materials, including hardness and mechanical strength, have led to their increased utilization in various industries. These materials are particularly attractive for industries that experience impact loading. Impact occurs when a body collides suddenly with a limited volume of material or structure. Polymer composites have gained popularity in sectors such as aerospace, construction, automotive, and defense, replacing traditional steel structures due to their favorable physical and mechanical properties [1-4]. It is crucial to understand the behavior of these materials under different loading conditions, including static and dynamic loads. Impact loading represents one of the complex forms of dynamic loading [5-7]. The primary reinforcements employed in composite structures designed to withstand high-velocity impacts are glass fibers, carbon fibers, Kevlar, and ultra-high molecular weight polyethylene fibers. Low-velocity impacts typically involve collision speeds ranging from 3 to 10 meters per second, with the Charpy and Izod devices commonly used to assess impacts within this speed range. The investigation of impact phenomena encompasses a wide range of velocities, with different evaluation methods employed for each speed regime [8-12]. For average velocity impacts ranging from 10 to 100 meters per second, free-fall impact devices and weights are utilized. Moving to high-velocity impacts, which occur between 100 and 1500 meters per second, devices such as gas guns or firearms are employed for evaluation. Finally, very high-velocity impacts falling within the range of 1500 to 15000 meters per second are evaluated using a two-stage gas gun that harnesses high-energy explosive materials [13-15].

The study of impact has provided insights into various material properties and outcomes associated with impacts, including heat generation, sound production, deformation, permanent damage, and projectile penetration. In the case of composite materials, the behavior under impact is influenced by factors such as the type of fiber and matrix materials used, testing methods employed, and fabrication techniques utilized. Composite materials exhibit increased resistance to impact loads when the impact aligns with the fibers' orientation. However, these materials are vulnerable to fracture when subjected to impacts in directions other than the fiber orientation [16-18]. Failure mechanisms observed in composites under impact loads include fiber fracture, fiber-matrix debonding, resin fragmentation, delamination between layers, and fiber pullout. The reduced impact resistance of composite materials can be attributed to factors such as low interlayer shear strength, limited plastic deformation, and delamination, which compromise the material's homogeneity. To ensure the reliable design and construction of composite structures and components capable of withstanding impacts, it is essential to have a comprehensive understanding of the material response under impact loading conditions [17-21]. This necessitates the use of various experimental techniques and sample designs. During an impact event, stress waves propagate in both the projectile and the target, generating compressive and shear stresses in the

thickness direction and tensile and shear stresses in the radial direction. The forces involved in impact include compressive, inertial, and frictional forces. In a scenario where a high-velocity projectile strikes a target, the target undergoes three stages. The first stage involves the initial contact between the projectile and the target, leading to material compression in both bodies. Assuming the projectile is rigid and significantly harder than the target, this compression propagates, initiating the second stage. Material flow occurs to a limited extent in the radial direction. The material flow continues until the compressive stress waves reach the back of the target, generating compressive stresses beneath the projectile region and subjecting the target to stress transformations. In the development of knee prostheses, advanced technologies and materials are utilized to enhance their performance and longevity. These include high-performance alloys like cobalt-chromium and titanium, which provide excellent mechanical properties and biocompatibility. Polyethylene with cross-linking techniques improves wear resistance, while ceramics such as zirconia and alumina offer exceptional hardness and strength. Computer-Aided Design (CAD) and 3D printing enable precise customization and patient-specific implants. Biomaterial coatings promote osseointegration, and sensor technology allows for adjustments based on joint movement and load distribution. Minimally invasive surgical techniques and robotic-assisted surgery improve implant placement and recovery. With these advancements, knee prostheses continue to improve in durability, functionality, and patient satisfaction, allowing individuals to regain mobility and actively engage in sports and physical activities. This study aims to enhance the chemical and mechanical stability of knee prostheses in orthopedic applications, specifically in sports-related use, through the development of ceramic nanoparticle-reinforced carbon nanocomposites. The novelty of this research lies in investigating the influence of nanoceramics on the mechanical behavior of hybrid epoxy/glass fiber composites under ballistic loading conditions. The mechanical properties, including elastic modulus, ultimate tensile strength, and flexural strength, will be assessed, along with the ballistic properties such as ballistic efficiency, ballistic limit velocities, and absorbed energy. By examining the performance of these nanocomposites, this study seeks to provide insights into their potential to enhance the stability and durability of knee prostheses in sports-related activities. The results will contribute to advancements in orthopedic materials and contribute to the design and development of improved knee prostheses for athletic individuals.

2. Materials and Methods

2.1. Materials and Processing for Toughened Epoxy Composites

The materials utilized in this research comprise Epon 828 epoxy resin, which is produced by Shell Chemical Company and possesses two epoxy groups per equivalent weight of epoxy. Various curing agents have been recommended for Epon 828 epoxy resin, and the most appropriate one is selected based on the intended application of the composite. In this study, Huntsman's D-400, a polyoxypropylene diamine with a molecular weight of 400, was chosen as the curing agent. The use of D-400 resulted in a lower density of crosslinking within the resin, which contributed to increased

toughness and a more suitable tensile modulus. The fabrication of fiberless specimens, which are crucial for evaluating the mechanical properties of the pure resin, involves the use of silicone rubber molds. These molds, composed of RTV3120 silicone with a specific hardener ratio, offer several advantages such as high dimensional accuracy, heat resistance, flexibility, and efficient heat transfer. To eliminate air bubbles, the resin prepared in the previous stage undergoes a 20-minute vacuum treatment in a vacuum oven at a temperature of 60°C. Subsequently, the bubble-free resin is poured into preheated silicone molds, followed by an additional 10-minute vacuum treatment to remove any trapped bubbles. The specimens are then cured at 80°C for 2.5 hours, followed by an additional 2.5 hours at 120°C.

2.2. Fabricating Fiberless Composite Specimens

The flowchart provided below illustrates the sequential steps involved in fabricating fiberless specimens. For this research, E-glass fibers were employed, which are widely used in the composite industry due to their affordability. The study incorporated 12 layers of E-glass with a density of 55.2 g/cm³ and a thickness of 200 µm. The resin composition consisted of epoxy resin EPON 828, the hardener Jeffamine D-400, and the nano ZnO Cloisite30B. The VARTM method utilized various laboratory materials and equipment including a glass mold, a flow medium, a heat-resistant release agent, a heat-resistant vacuum bag, connecting hoses, valves, heat-resistant sealing tape, a vacuum pump, a resin trap, a thermometer, a pressure gauge, a scale, an oven, a vacuum oven, a stirrer, and a hot plate. Uniaxial tensile testing is a commonly employed method to assess the mechanical properties of materials, including composite materials.

2.3. Characterization of Layered Composites

The mechanical behavior of layered composites relies on the tensile forces experienced by each layer, which are characterized by parameters such as the tensile modulus, Poisson's ratios, and strength. Through the tensile test, it is possible to determine the tensile modulus, Poisson's ratios, tensile strength, and ultimate strain of composite materials. The testing procedure adheres to the ASTM D3039 standard, with the grips of the Instron 5500R machine moving at a rate of 2 mm per minute in the tensile direction. To prevent sample slippage, the mechanical grips are equipped with serrated surfaces. Uniaxial strain gauges are utilized for strain measurement. Standard tensile samples are prepared according to the specified guidelines, and reinforcing tabs are strategically placed at the regions where force is applied to the sample. These tabs facilitate proper force transfer, reinforce the sample, and reduce stress concentration between the grip and sample surfaces. However, the presence of tabs introduces a new stress concentration due to the abrupt change in thickness at the end, which can be mitigated by notching the end.

3. Results and Discussion

3.1. Advancements in Knee Prostheses

Since the early 1960s, there has been an increasing utilization of composite materials in structural applications due to their notable efficiency. However, recent research has focused on investigating

materials such as fiber-reinforced polymers, which require specific considerations to accurately determine their physical and mechanical properties. Knee prostheses play a crucial role in orthopedic applications, particularly in the context of sports-related injuries. Athletes often experience significant stress and strain on their knees due to the rigorous physical demands of sports activities. In cases where knee injuries or degenerative conditions compromise joint function, knee prostheses offer a viable solution to restore mobility, alleviate pain, and enable athletes to return to their sporting activities. These prosthetic devices are designed to replicate the natural structure and function of the knee joint, providing stability, range of motion, and weight-bearing capabilities. Advanced technologies and materials are employed in the development of knee prostheses, ensuring durability, longevity, and compatibility with the biomechanics of sports movements. By utilizing knee prostheses in orthopedic applications, sports-related injuries can be effectively managed, allowing athletes to resume their athletic pursuits with enhanced joint function and improved quality of life.

3.2. Testing Challenges and Manufacturing Strategies for Composite Materials

The aerospace industry has played a significant role in advancing composite material technology, with each aircraft manufacturer devising their own testing approaches due to the lack of standardized testing methods. The introduction of materials like boron, carbon fibers, Kevlar, epoxies, and polyamides further complicated the testing process, as existing methods may not be suitable for newly evaluated materials. Consequently, various testing methods have been developed to measure specific properties, but they often have constraints or complexities. Efforts have been made by organizations like ASTM to uphold existing standards and address general issues, but challenges persist. Meanwhile, research has focused on the manufacturing process of layered composites with a polymer matrix, aiming to achieve desirable properties through suitable physical and chemical interactions. Various methodologies have been explored to ensure complete impregnation and low porosity in the polymer matrix, including the dispersion of nanolayers within the epoxy. Two methods, solution mixing with acetone as a solvent and direct mixing, have been employed for dispersing ZnO within the epoxy to achieve the desired efficiency of the epoxy/ZnO nanocomposite. During the initial stage, it is crucial to establish the purpose and mission of the fabricated component within its operational context, particularly focusing on its structural applications. Successful outcomes rely on the chemical and thermodynamic compatibility of the components [21-23]. The interaction between polymer chains and surface modifiers on ZnO platelets plays a critical role in platelet opening, while incompatibility leads to platelet reorientation and undesired re-agglomeration during the dispersion of nano-ZnO and the curing process.

3.3. Advancements in Nanocomposites and Impact Behavior

The molecular weight of the resin affects the diffusion rate of resin chains into the ZnO platelets, with higher molecular weights resulting in slower diffusion. Additionally, the curing time of the hardener and the length of the hardener molecules influence the dispersion of nanoparticles and the exfoliation of ZnO platelets [24-28]. Recent years have witnessed significant attention towards the utilization of

nanocomposites due to their unique properties and potential applications. This literature review provides an overview of recent studies that focus on the incorporation of nanocomposites, particularly in the fields of materials science and electrochemical sensors. Extensive research has been conducted on the impact behavior and damage in composite materials, including the dynamic response of composite sandwich panels to low-velocity impact [29-30]. Studies have also examined the ballistic impact behavior of woven fabric composites, analyzing the impact response under various parameters [31-33]. Numerical modeling has played a crucial role in understanding the behavior of sandwich panels and assessing the impact resistance of composite structures [34-35]. Furthermore, investigations have been carried out on the crush behavior of honeycomb cores [36], the impact behavior of composite laminates with delamination's [38-39], and the response of various composite materials to low-velocity impact [40-41]. High-velocity impact and perforation behavior of polymer composite laminates have been explored [42-43], along with the ballistic perforation of planar plain-woven fabric targets [44]. The incorporation of nanoparticles in composites has shown promise in enhancing impact resistance [45], and the behavior of nanostructured laminated plates under low-velocity impact has been investigated [46]. Collectively, these studies contribute to the understanding of impact behavior and damage mechanisms in composite materials, offering valuable insights for their design and optimization. Moshayedi et al. [49] focused their research on the development of a multi-nano sensor based on graphene oxide/polyaniline nanocomposite. The sensor demonstrated the ability to simultaneously detect carbon dioxide, methane, ethanol, and ammonia gases. Their study showed the versatility of nanocomposite-based sensors in gas detection applications, showcasing potential advancements in environmental monitoring and safety. Yousefi et al. [50] conducted a statistical evaluation to assess relevant parameters in the bio-synthesis of Ag/MWF-CNT composites using the Plackett-Burman design and response surface methodology. Their study emphasized the significance of optimizing synthesis parameters in the fabrication of nanocomposites, contributing to the understanding of factors that influence the properties of these materials. Azin et al. [51] developed an electrochemical sensor by utilizing a nanocomposite electrode composed of multi-walled carbon nanotubes (MWCNTs), TiO_2, and a carbon ionic liquid. The sensor was specifically designed for the analysis of acetaminophen in pharmaceutical formulations. Their study highlighted the potential of nanocomposite electrodes in pharmaceutical analysis, offering improved sensitivity and selectivity for drug detection.

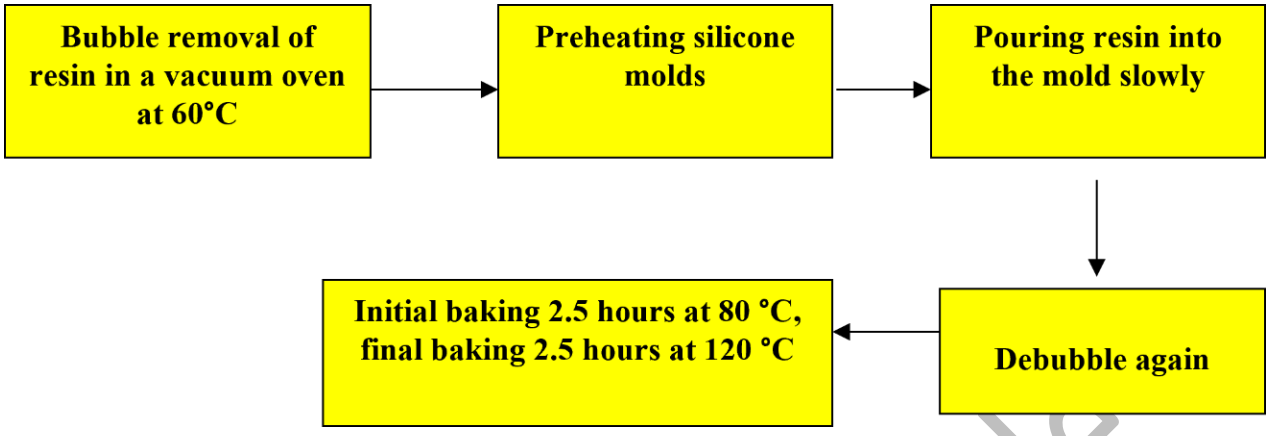

Figure 1: Fabrication process of fibreless specimens

The elimination of bubbles is of utmost importance during the fabrication of these specimens. The presence of residual bubbles within the specimens, as depicted in Figure 1, indicates that they were not completely removed prior to the curing process. It is crucial to carefully control the vacuum conditions to avoid a decrease in pressure and an increase in temperature within the vacuum oven. Such conditions can result in resin boiling and the formation of minuscule bubbles that may not be readily detectable but can have a substantial detrimental impact on the mechanical properties.

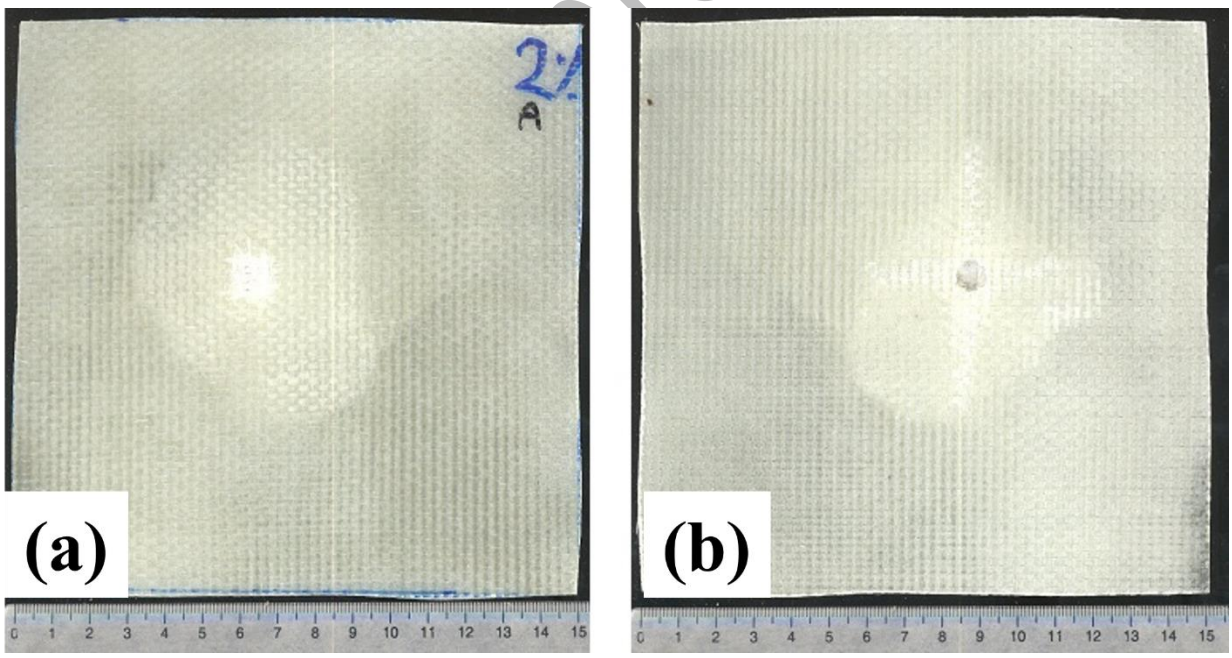

Figure 2: 7% sample exhibiting incomplete mold filling due to high resin viscosity

3.4. Tensile Testing Procedure and Projectile Launching Safety Measures

The testing procedure depicted in Figure 2 follows the guidelines outlined in the ASTM D3039 standard for tensile testing. The grips of the Instron 5500R machine move at a constant rate of 2 mm per minute in the direction of tension. To ensure the stability of the test samples and prevent slippage during the

experiment, the mechanical grips are equipped with serrated surfaces that provide additional grip and traction. For accurate strain measurement, uniaxial strain gauges are employed. These strain gauges are designed to detect and quantify the deformation or elongation of the test specimens under tensile loading. By adhering to the ASTM D3039 standard and implementing appropriate grip surfaces and strain measurement techniques, the testing procedure aims to ensure reliable and consistent results in evaluating the mechanical properties of the materials being tested. During the experimental procedure, the projectile was launched at a high velocity without precise control over its trajectory. To mitigate potential hazards, all operations were conducted within a sealed steel enclosure to prevent collisions and damage. Compacted waxes were employed as a means to arrest the projectile's motion after passing through the specimen. A chronograph, equipped with laser sensors, was utilized to measure the time taken by the projectile to travel between them.

3.5. Velocity Measurement and Pressure-Velocity Curve

The velocity readings were initially displayed in feet per second (ft/s) and subsequently converted to meters per second (m/s). However, ensuring the accurate positioning of the chronograph in each test posed a challenge. The pressure behind the projectile was adjusted based on the desired velocity ratios, taking into account factors such as barrel length, projectile weight, and gas reservoir type. Pressure-velocity curves were established for each projectile by substituting the fixture and aluminum foil panels with the chronograph and conducting multiple shots at different pressures.

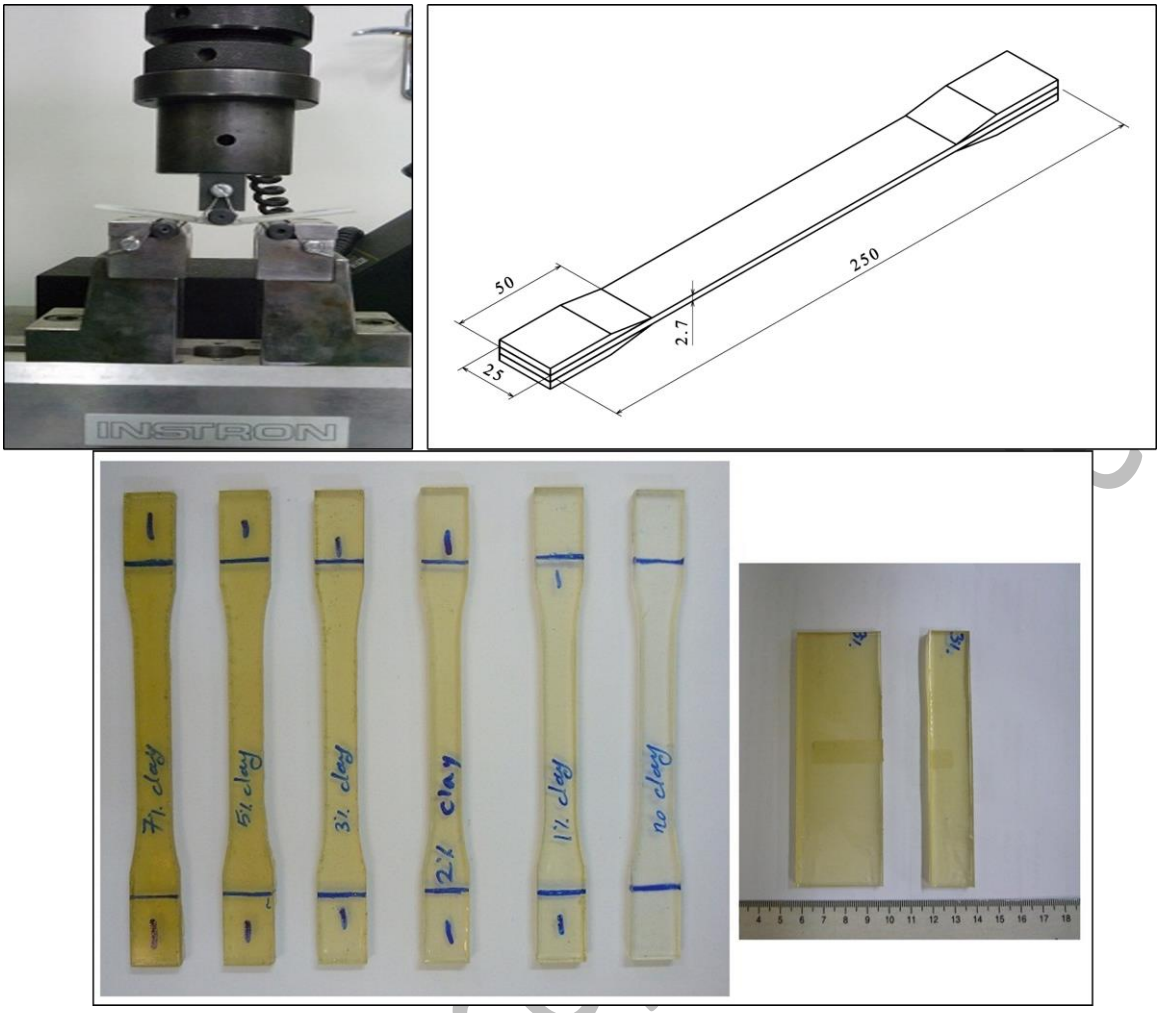

Figure 3: Schematic and dimensions of tensile test samples (all dimensions are in mm)

By averaging the velocities obtained for each pressure, the corresponding pressure values were determined. This iterative process was repeated for various pressures to obtain comprehensive pressure-velocity curves. In subsequent experiments, the chronograph was no longer employed, and the pressure behind the projectile was adjusted based on the desired velocity using the established curves. To measure the exit velocity, a high-speed counter was utilized. The projectile penetrated two aluminum foil panels positioned on opposite sides of a target panel, thereby establishing electrical connections between the wires attached to them and initiating the counter. Upon piercing the first panel, the projectile punctured the aluminum foil panels of the second panel, further connecting the wires and deactivating the counter. The counter displayed the calculated time, which, in conjunction with the distance between the puncture holes on the panels, was used to determine the exit velocity. Figure 3 shows a schematic representation of the tensile test samples along with their corresponding dimensions, expressed in millimeters (mm). The purpose of this figure is to provide a visual depiction of the geometry and size of the test specimens used in the tensile testing procedure. By including the dimensions, it allows researchers and readers to have a clear understanding of the physical attributes of the samples, aiding in the replication and interpretation of the experimental setup. The schematic

illustration assists in visualizing the overall shape and configuration of the test samples, while the accompanying numerical values provide precise measurements for length, width, thickness, or any other relevant dimensions that are crucial for accurately conducting and evaluating the tensile tests. It is essential to acknowledge that the data presented in Table 1 was obtained from experiments conducted in the X-ray scattering laboratory. However, the specific methodology used to calculate the data is not specified. Upon examining Table 1, it becomes evident that the samples prepared using the initial approach, which involves dissolution in acetone solvent, exhibit a flake-like morphology, except for the 7% sample, which displays a distinct peak.

Table 1: XRD results for samples with two manufacturing methods

Construction / Percentage of nanoceramics / method	%1		%2		%3		%5		%7	
	2θ	d* (Å)	2θ	d (Å)	2θ	d (Å)	2θ	d (Å)	2θ	d (Å)
Solution mixing method		-	-	-	-	-	-	-	2.22	40.76
Direct mixing method	2.18	40.86	2.09	44.36	1.26	40.39	2.11	4234	2.18	40.52

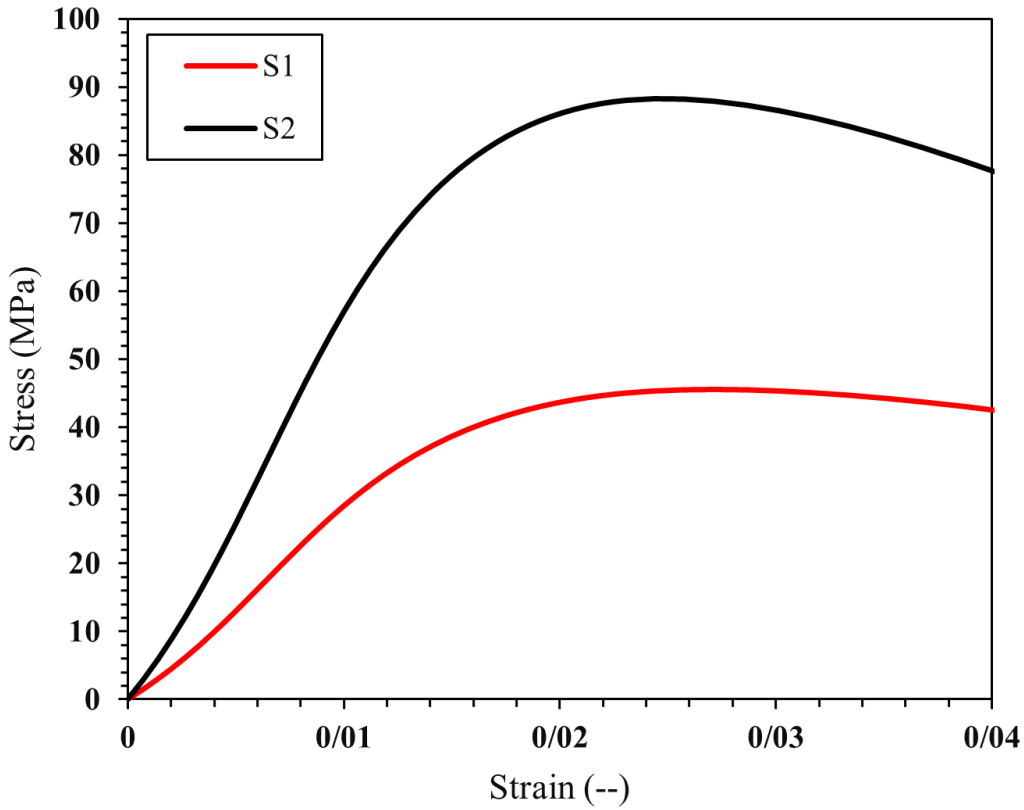

Figure 4: Strain stress diagram for the resin sample with 5-7% nanoceramic and with two different manufacturing methods

3.6. Mechanical Property Comparison and Fabrication of Hybrid Resin

The stress-strain diagram presented in Figure 4 shows clear evidence that the samples prepared using the second method exhibit superior ultimate strength and elongation. It is important to note that the stress-strain diagram can be derived from the force-displacement diagram, which is also provided by the tensile testing equipment, given the knowledge of the sample's surface area. This improvement in

mechanical properties can be attributed to the incomplete removal of acetone solvent from the mixture, which negatively affects the mechanical characteristics. Table 2 compares the mechanical properties of two sets of 2% ceramic nanoparticle samples prepared using both methods with a pure resin sample that does not contain nanoparticles. The results highlight the enhanced mechanical properties of the resin samples prepared using the second method. Considering the simplicity and efficiency of this approach, as well as the improved mechanical properties observed, the hybrid resin samples were fabricated using the second method and subsequently subjected to mechanical and impact assessments.

Table 2: Mechanical properties of the pure sample and samples reinforced with nanoceramic

	The percentage of length increase	**Ultimate strength (MPa)**	**Elastic modulus (GPa)**
Pure sample	**4.5**	**55.9**	**3.3**
Solution mixing method	**2.1**	**59.63**	**3.69**
Direct mixing method	**3.56**	**95.65**	**4.59**

Table 2 shows a comparison of the mechanical properties between the pure sample and the samples reinforced with nanoceramic. The pure sample exhibits an elastic modulus of 3.3 GPa, ultimate strength of 55.9 MPa, and a length increase of 4.5%. The sample prepared using the solution mixing method demonstrates an increased elastic modulus of 3.69 GPa, ultimate strength of 59.63 MPa, and reduced length increase of 2.1%. In contrast, the direct mixing method yields further improvements, with an elastic modulus of 4.59 GPa, ultimate strength of 95.65 MPa, and length increase of 3.56%. Both methods of nanoceramic reinforcement show enhanced mechanical properties compared to the pure sample. The direct mixing method exhibits the highest enhancement, characterized by significant increases in elastic modulus and ultimate strength. Additionally, both reinforced samples display lower length increases, indicating improved dimensional stability. These findings underscore the effectiveness of nanoceramic reinforcement in enhancing the mechanical properties of the resin matrix, with the direct mixing method proving particularly successful in achieving superior mechanical performance. In high-velocity impacts of composite targets, the fragmentation mechanism involves a combination of spallation and petaling phenomena. Spallation refers to the separation of the target material from the projectile due to the presence of a high shear strain band near the projectile radius. On the other hand, petaling occurs as a result of the formation of radial and rotational cracks caused by the impact of the projectile. Various factors contribute to deviations in the trajectory of the projectile after penetrating the target, including the non-homogeneity of the target material, imperfect perpendicular entry of the projectile, the projectile missing the center of the target, and the uneven growth of petal-like fragments.

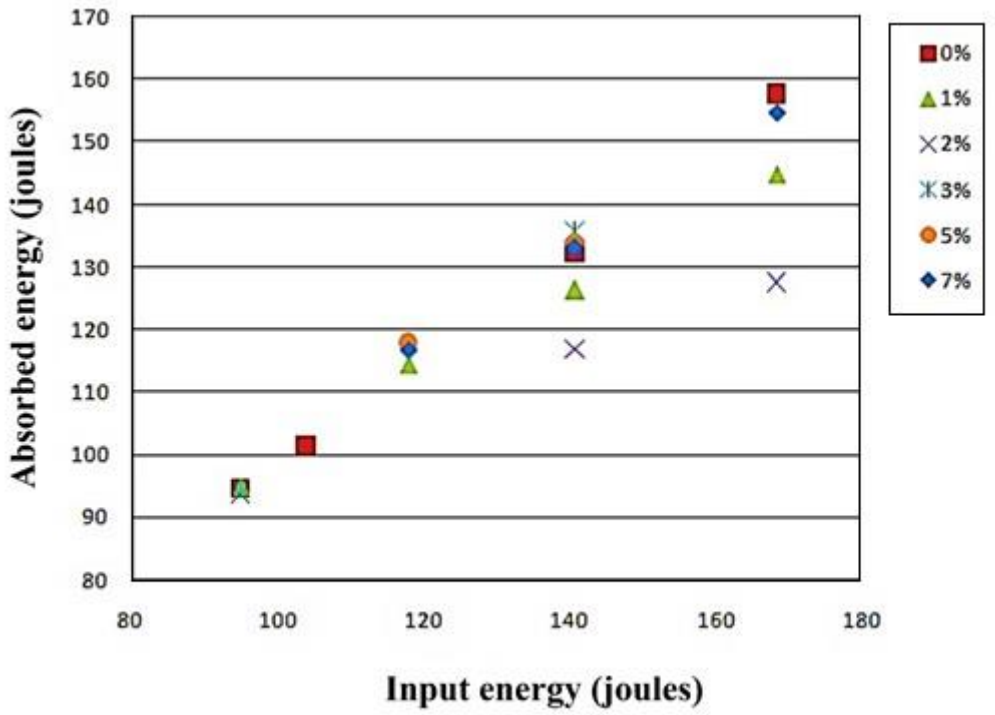

Figure 5: Absorbed energy in terms of projectile input energy

The relationship between input energy and output energy for different nanowire percentages is depicted in Figure 5. Increasing the input energy leads to a higher energy absorption by the target, which can be attributed to the strain rate sensitivity of glass fibers. The absorption rate of energy also rises with impact velocity, indicating the positive impact of strain rate on the energy absorption of glass-epoxy composites. Comparative analysis among different composite materials reveals that glass-fiber reinforced composites exhibit a higher dynamic enhancement factor compared to carbon-fiber or Kevlar-fiber reinforced composites. The dynamic effects become more pronounced as the degree of target damage or fragmentation increases. Typically, the absorbed energy corresponds to approximately half the difference between the input and output kinetic energies, as shown in Figure 5.

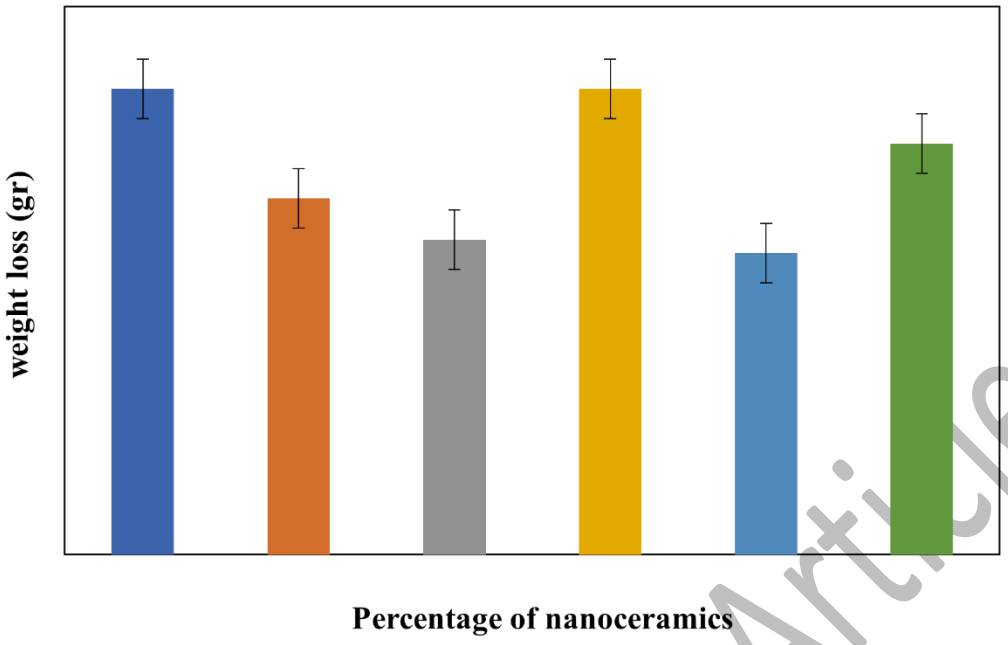

Figure 6: Target weight reduction after projectile impact

3.7. Influence of Nano ZnO on Damage Mechanisms

In the conducted experiments, various parameters such as material properties, target hardness, bullet specifications, layering, structure of layers, preloading, and environmental conditions were identified as influencing factors affecting the type and extent of damage. However, in these experiments, only material properties and target hardness were deliberately manipulated, while other parameters were kept constant throughout. Fracture of resin and fibers represents a localized mechanism of damage. To assess and compare this type of damage, the weight of the target samples was measured before and after impact testing. Figure 6 illustrates the weight reduction of the target samples following projectile impact, which includes fiber fragmentation, resin fragmentation, and plugging. The results indicate that the inclusion of nano ZnO enhances the ballistic performance of the structure by increasing the projectile's energy absorption. However, it also results in a larger area of damage, potentially hindering the structure's ability to fulfill its intended mission after impact due to the extent of damage sustained. In summary, the impact of nano ZnO should be evaluated considering the structure's mission, to determine whether it can continue functioning after impact or if it requires replacement with another component. These images also show a notable shift in the fracture mode from interlayer to intralayer. The addition of nano ZnO increases the brittleness between layers but reduces the adhesion between the resin and fibers. However, when the nano ZnO content exceeds a certain threshold (beyond 5%), the remaining agglomerates within the resin decrease interlayer brittleness, and at the same time, interlayer adhesion continues to decline. As a result, this leads to the emergence of a combined fracture mode characterized by multiple delamination and intralayer fracture in the 7% sample. Figure 7 presents cross-sectional views of samples with varying concentrations (0%, 3%, and 7%) of nanoceramics after experiencing projectile penetration.

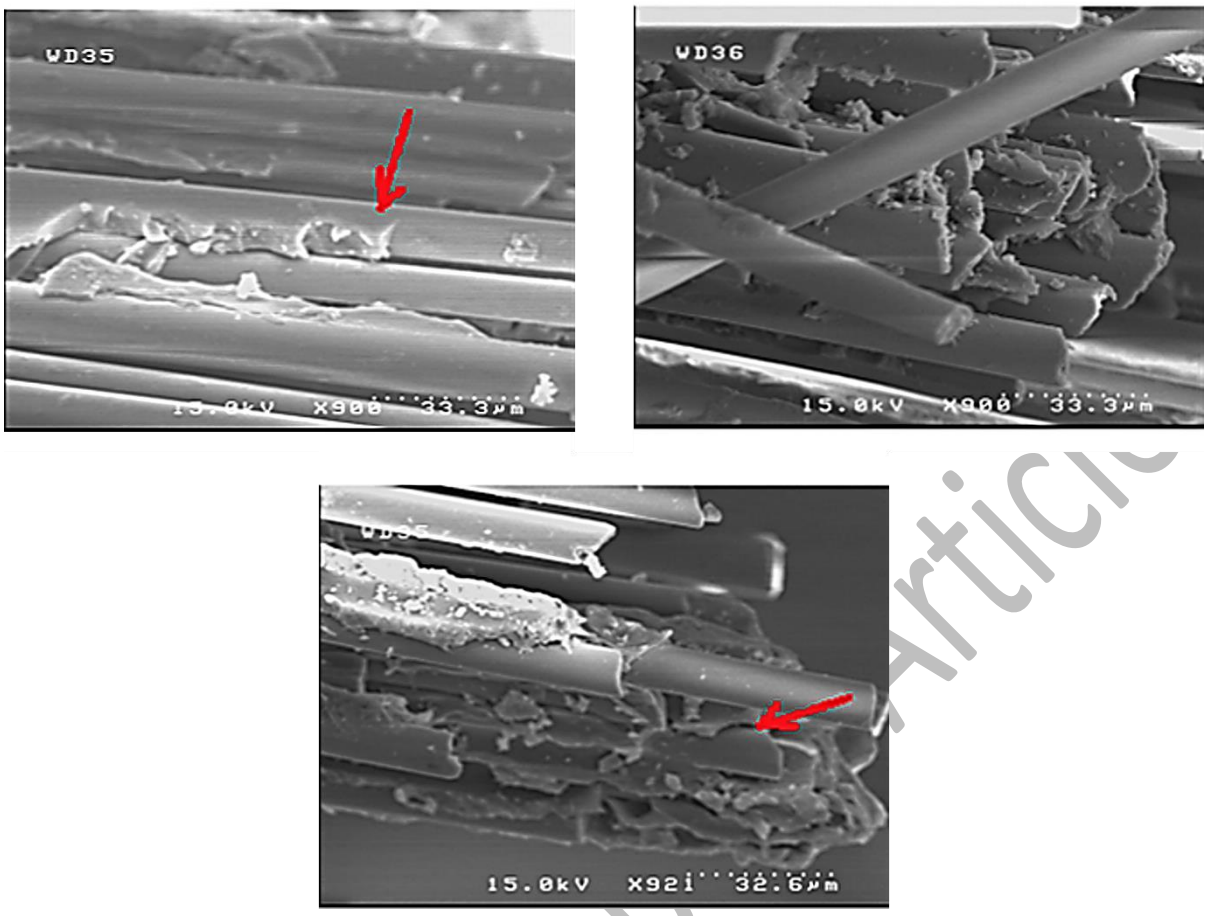

Figure 7: SEM photo of the cross section of the samples, a) 0%, b) 3% and c) 7%. The ratio of cut fiber thickness to stretched fiber thickness in the sample is 7% less than the other two samples.

The visual evidence provides clear confirmation of complete delamination beneath a specific layer, leading to the formation of a plug, as well as partial delamination occurring across different layers with varying extents. The thickness of the plug can be determined by examining sectioned layers. In the absence of nanoceramics (Figure 7a), the plug is relatively thinner, and fewer occurrences of interlayer delamination are observed. In contrast, in the sample with 1% nanoceramics (Figure 7b), the plug exhibits increased thickness, resulting in a reduced occurrence of fiber breakage due to decreased tensile stress. Multiple interlayer delaminations are visible; however, their areas are reduced due to the favorable brittleness of the matrix. Notably, the cross-section of the 7% sample (Figure 7c) displays more pronounced delamination and internal intralayer damage, which can be attributed to the weak adhesion between the fibers and matrix. These factors, combined with significant target deformation arising from its low flexural stiffness, contribute to higher energy absorption compared to the 1% sample. The composite material consisting of single-walled carbon nanotubes (SWCNT) and zinc oxide (ZnO) shows significant potential for sport applications in the athletic field. This composite offers several advantageous properties for athletes, including exceptional strength, lightweight characteristics, and high electrical conductivity attributed to the SWCNT component. The inclusion of ZnO further improves the composite by providing antibacterial and UV-blocking properties, which are essential for maintaining hygiene and protecting against harmful radiation during outdoor activities. Additionally,

the SWCNT-ZnO composite demonstrates enhanced thermal management capabilities, ensuring efficient heat dissipation and reducing the risk of overheating during intense physical exertion. By adjusting the composition and processing parameters, the composite can be tailored to specific sport applications, offering improved performance, comfort, and protection for athletes. The SWCNT-ZnO composite shows great promise in enhancing athletic performance and safety, making it an appealing choice for various sport-related uses.

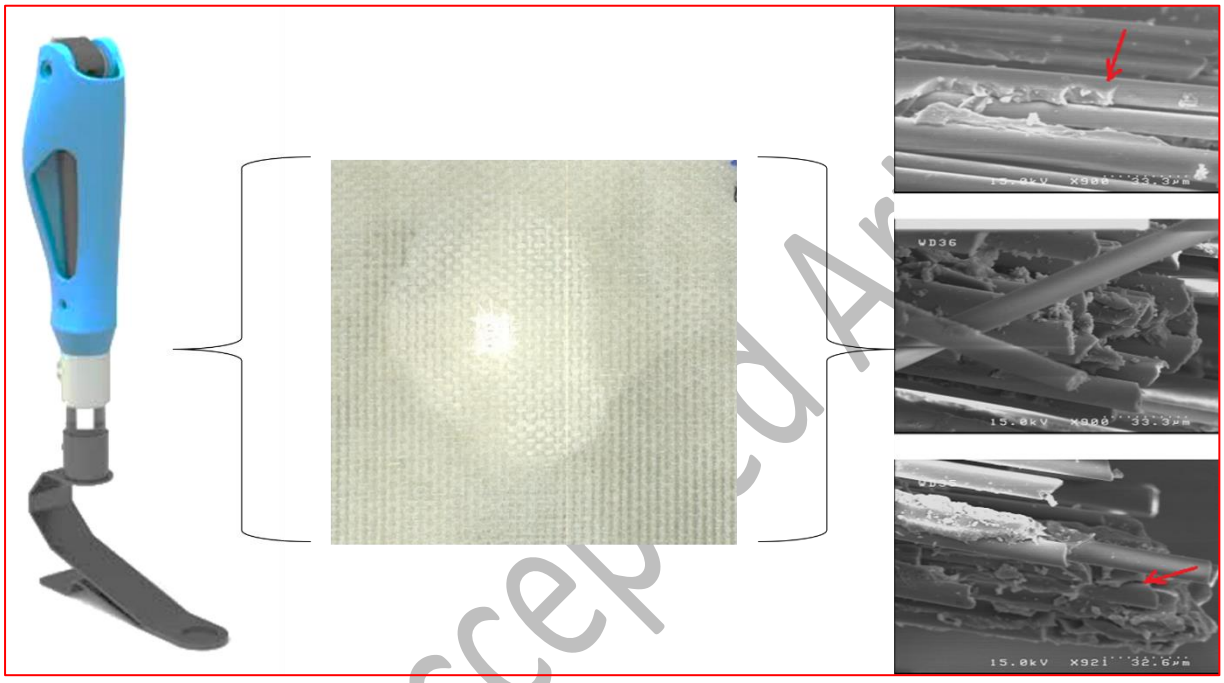

Figure 8: Presentation of the mechanical properties of Carbon Fiber Reinforced Polymer (CFRP) composites used for sport applications

3.8. CFRP Composites for Sport-Related Application

Figure 8 shows the mechanical properties of Carbon Fiber Reinforced Polymer (CFRP) composites specifically developed and utilized for sport-related applications. These composites are constructed by incorporating carbon fibers within a polymer matrix, resulting in a material that exhibits exceptional strength, stiffness, and durability, making it highly suitable for demanding athletic activities. Figure 8 presents essential insights into the performance characteristics of CFRP composites, shedding light on their suitability for various structural applications. Figure 8 includes valuable data on key mechanical properties such as tensile strength, compressive strength, flexural strength, Young's modulus, and impact resistance. The results highlight the remarkable load-bearing capabilities and strength of CFRP composites, as evidenced by their high values of tensile, compressive, and flexural strengths [51-54]. The stiffness of CFRP composites, as indicated by the Young's modulus values, makes them well-suited for applications that require rigidity and structural integrity. Moreover, the CFRP composites exhibit excellent resistance to impacts, demonstrating their ability to withstand sudden and high-energy impacts

without experiencing failure. These exceptional mechanical properties establish CFRP composites as a compelling alternative to traditional materials, offering a superior strength-to-weight ratio and enhanced resistance to corrosion. Figure 8 serves as a valuable resource for researchers, engineers, and designers involved in the optimization and application of CFRP composites, facilitating the selection of suitable materials and enhancing understanding of their behavior under different loading conditions.

4. Conclusion

The research results suggest that the Vacuum Assisted Resin Transfer Molding (VARTM) method is suitable for the production of hybrid nanocomposites, provided certain factors are taken into consideration, such as the number of channels, mold temperature, and resin temperature. It is recommended to inject the resin immediately after dispersing carbon nanofiber and nanoceramics into the epoxy to prevent premature resin curing. The second production method demonstrated significant enhancements in tensile strength and elastic modulus compared to the first method, likely due to incomplete removal of residual solvents. Hybrid samples containing 3% carbon nanofiber and nanoceramics showed increased tensile strength and elastic modulus. Additionally, flexural strength and modulus improved with the incorporation of carbon nanofiber and nanoceramics. The inclusion of carbon nanofiber and nanoceramics also resulted in an increased ballistic limit velocity. Further recommendations include exploring other types of nanofillers, integrating Kevlar and carbon fibers into the composite, conducting comprehensive mechanical tests, performing compression and ballistic impact tests, assessing crack propagation resistance, considering the use of rubber epoxy, and employing numerical modeling techniques for optimization. Based on the investigations and research presented in this article, it can be concluded that VARTM is a suitable method for producing hybrid nanocomposites, provided specific considerations are taken into account, such as the appropriate number of inlet and outlet channels, suitable mold temperature, and appropriate resin temperature. To prevent premature resin curing when using high percentages of carbon nanofiber and nanoceramics during the initial stage of the molding process, it is recommended to inject the resin immediately after dispersing the carbon nanofiber and nanoceramics into the epoxy, as these materials possess hardening properties. The resin temperature should not exceed 80°C before molding, and a short mixing time of less than 10 minutes at high speed is advised. The second production method demonstrated significant improvements in the tensile strength and elastic modulus of the samples, with increases of 60% and 21%, respectively, compared to the samples produced by the first method. These results suggest that residual solvents may not have been completely removed from the resin, significantly affecting its properties. Hybrid samples containing 3% carbon nanofiber and nanoceramics showed improvements of 11% in tensile strength and 15% in elastic modulus compared to samples without them. The flexural strength of the sample with 3% carbon nanofiber and nanoceramics increased by 11% compared to the sample without them, while the flexural modulus of the sample with 5% carbon nanofiber and nanoceramics demonstrated a significant improvement of 48%. Furthermore, the inclusion of 5% and

7% carbon nanofiber and nanoceramics resulted in a ballistic limit velocity of 130 m/s, which was 12% higher than the velocity of the control sample (116 m/s).

5. Reference

[1] Tan, V. B. C., Lim, C. T., & Cheong, C. H. (2003). Perforation of high-strength fabric by projectiles of different geometry. *International Journal of Impact Engineering*, *28*(2), 207-222.

[2] Tan, V. B. C., & Khoo, K. J. L. (2005). Perforation of flexible laminates by projectiles of different geometry. *International Journal of Impact Engineering*, *31*(7), 793-810.

[3] Brunner, A. J., Necola, A., Rees, M., Gasser, P. H., Kornmann, X., Thomann, R., & Barbezat, M. (2006). The influence of silicate-based nano-filler on the fracture toughness of epoxy resin. Engineering fracture mechanics, 73(16), 2336-2345.

[4] Akbari-Aghdam, H., Bagherifard, A., Motififard, M., Parvizi, J., Sheikhbahaei, E., Esmaeili, S., ... & Khandan, A. (2021). Development of porous photopolymer resin-SWCNT produced by digital light processing technology using for bone femur application. *Archives of Bone and Joint Surgery*, *9*(4), 445.

[5] Haque, A., Shamsuzzoha, M., Hussain, F., & Dean, D. (2003). S2-glass/epoxy polymer nanocomposites: manufacturing, structures, thermal and mechanical properties. *Journal of Composite materials*, *37*(20), 1821-1837.

[6] McKnight, D. H., Choudhury, V., & Kacmar, C. (2002). The impact of initial consumer trust on intentions to transact with a web site: a trust building model. *The journal of strategic information systems*, *11*(3-4), 297-323.

[7] Lin, L. Y., Lee, J. H., Hong, C. E., Yoo, G. H., & Advani, S. G. (2006). Preparation and characterization of layered silicate/glass fiber/epoxy hybrid nanocomposites via vacuum-assisted resin transfer molding (VARTM). *Composites Science and Technology*, *66*(13), 2116-2125.

[8] Karaki, T., Killgore, J. P., & Seferis, J. C. (2004, May). Characterization of fatigue behavior of polynanomeric matrix composites. In *CD proceeding of 49th International Sample Symposium and Exhibition*.

[9] Wang, K., Chen, L., Wu, J., Toh, M. L., He, C., & Yee, A. F. (2005). Epoxy nanocomposites with highly exfoliated clay: mechanical properties and fracture mechanisms. *Macromolecules*, *38*(3), 788-800.

[10] Siddiqui, N. A., Woo, R. S., Kim, J. K., Leung, C. C., & Munir, A. (2007). Mode I interlaminar fracture behavior and mechanical properties of CFRPs with nanoclay-filled epoxy matrix. Composites Part A: Applied science and manufacturing, 38(2), 449-460.

[11] Ngo, T. D., Ton- That, M. T., Hoa, S. V., & Cole, K. C. (2008). Reinforcing effect of organoclay in rubbery and glassy epoxy resins, part 1: Dispersion and properties. *Journal of Applied Polymer Science*, *107*(2), 1154-1162.

[12] Peila, R., Seferis, J. C., Karaki, T., & Parker, G. (2009). Effects of nanoclay on the thermal and rheological properties of a VARTM (vacuum assisted resin transfer molding) epoxy resin. *Journal of thermal analysis and calorimetry*, *96*, 587-592.

[13] Ngo, T. D., Ton-That, M. T., Hoa, S. V., & Cole, K. C. (2009). Effect of temperature, duration and speed of pre-mixing on the dispersion of clay/epoxy nanocomposites. *Composites Science and Technology*, *69*(11-12), 1831-1840.

[14] Saharudin, M. S., Jumahat, A., Kahar, A. Z., & Ahmad, S. (2013). The influence of alumina filler on impact properties of short glass fiber reinforced epoxy. *Applied Mechanics and Materials*, *393*, 88-93.

[15] V. Tan, C. Lim, and C. Cheong, "Perforation of high-strength fabric by projectiles of different geometry," International Journal of Impact Engineering, vol. 28, pp. 207-222, 2003.

[16] Eskizeybek, V., Avci, A., & Gülce, A. (2014). The Mode I interlaminar fracture toughness of chemically carbon nanotube grafted glass fabric/epoxy multi-scale composite structures. *Composites Part A: Applied Science and Manufacturing*, *63*, 94-102.

[17] Safaei, M. M., Abedinzadeh, R., Khandan, A., Barbaz-Isfahani, R., & Toghraie, D. (2023). Synergistic effect of graphene nanosheets and copper oxide nanoparticles on mechanical and thermal properties of composites: Experimental and simulation investigations. *Materials Science and Engineering: B*, *289*, 116248.

[18] Wicks, S. S., de Villoria, R. G., & Wardle, B. L. (2010). Interlaminar and intralaminar reinforcement of composite laminates with aligned carbon nanotubes. *Composites Science and Technology*, *70*(1), 20-28.

[19] Davis, D. C., & Whelan, B. D. (2011). An experimental study of interlaminar shear fracture toughness of a nanotube reinforced composite. *Composites Part B: Engineering*, *42*(1), 105-116.

[20] Seyhan, A. T., Tanoglu, M., & Schulte, K. (2008). Mode I and mode II fracture toughness of E-glass non-crimp fabric/carbon nanotube (CNT) modified polymer based composites. *Engineering Fracture Mechanics*, *75*(18), 5151-5162.

[21] Wichmann, M. H., Sumfleth, J., Gojny, F. H., Quaresimin, M., Fiedler, B., & Schulte, K. (2006). Glass-fibre-reinforced composites with enhanced mechanical and electrical properties–benefits and limitations of a nanoparticle modified matrix. *Engineering fracture mechanics*, *73*(16), 2346-2359.

[22] Bashar, M. T., Sundararaj, U., & Mertiny, P. (2013). Mode-I interlaminar fracture behaviour of nanoparticle modified epoxy/basalt fibre-reinforced laminates. *Polymer Testing*, *32*(2), 402-412.

[23] Tang, Y., Ye, L., Zhang, D., & Deng, S. (2011). Characterization of transverse tensile, interlaminar shear and interlaminate fracture in CF/EP laminates with 10 wt% and 20 wt% silica nanoparticles in matrix resins. *Composites Part A: Applied Science and Manufacturing*, *42*(12), 1943-1950.

[24] Monfared, R. M., Ayatollahi, M. R., & Isfahani, R. B. (2018). Synergistic effects of hybrid MWCNT/nanosilica on the tensile and tribological properties of woven carbon fabric epoxy composites. *Theoretical and Applied Fracture Mechanics*, *96*, 272-284.

[25] Ayatollahi, M. R., Barbaz Isfahani, R., & Moghimi Monfared, R. (2017). Effects of multi-walled carbon nanotube and nanosilica on tensile properties of woven carbon fabric-reinforced epoxy composites fabricated using VARIM. *Journal of Composite Materials*, *51*(30), 4177-4188.

[26] Mathivanan, N. R., & Jerald, J. (2012). Interlaminar fracture toughness and low-velocity impact resistance of woven glass epoxy composite laminates of EP3 grade. *Journal of Minerals and Materials Characterization and Engineering*, *11*(03), 321.

[27] Moroni, F., Palazzetti, R., Zucchelli, A., & Pirondi, A. (2013). A numerical investigation on the interlaminar strength of nanomodified composite interfaces. *Composites Part B: Engineering*, *55*, 635-641.

[28] Tan, V. B. C., & Khoo, K. J. L. (2005). Perforation of flexible laminates by projectiles of different geometry. *International Journal of Impact Engineering*, *31*(7), 793-810.

[29] Goldsmith, W., & Sackman, J. L. (1992). An experimental study of energy absorption in impact on sandwich plates. *International Journal of Impact Engineering*, *12*(2), 241-262.

[30] Fatt, M. S. H., & Park, K. S. (2001). Dynamic models for low-velocity impact damage of composite sandwich panels–Part A: Deformation. *Composite Structures*, *52*(3-4), 335-351.

[31] Naik, N. K., Shrirao, P., & Reddy, B. C. K. (2006). Ballistic impact behaviour of woven fabric composites: Formulation. *International journal of impact engineering*, *32*(9), 1521-1552.

[32] Attaeyan, A., Shahgholi, M., & Khandan, A. (2023). Fabrication and characterization of novel 3D porous Titanium-6Al-4V scaffold for orthopedic application using selective laser melting technique. Iranian Journal of Chemistry and Chemical Engineering.

[33] Naik, N. K., & Shrirao, P. (2004). Composite structures under ballistic impact. *Composite structures*, *66*(1-4), 579-590.

[34] Kepler, J. A., & Hansen, M. R. (2007). Numerical modeling of sandwich panel response to ballistic loading—energy balance for varying impactor geometries. *Journal of Sandwich Structures & Materials*, *9*(6), 553-570.

[35] Hu, Z., Zhou, C., Ni, Z., Lin, X., & Li, R. (2023). New symplectic analytic solutions for buckling of CNT reinforced composite rectangular plates. *Composite Structures*, *303*, 116361.

[36] Çelik, M., Güden, M., Sarıkaya, M., Taşdemirci, A., Genç, C., Ersoy, K., & Serin, Ö. (2023). The impact response of a Nomex® honeycomb core/E-glass/epoxy composite sandwich structure to increasing velocities: experimental and numerical analysis. *Composite Structures*, 117205.

[37] Yuan, L., Liang, S., & Yan, S. (2023). In-Plane Elastic Properties of Stitched Plain Weave Composite Laminate. *Journal of Shanghai Jiaotong University (Science)*, *28*(2), 220-232.

[38] Karmakar, S., Bandyopadhyay, T., & Karmakar, A. (2023). Transient Behaviour and Impact Induced First-Ply Failure of Delaminated Composite Conical Shells. *Journal of Vibration Engineering & Technologies*, 1-23.

[39] Moharana, A. P., Raj, R., & Dixit, A. R. (2023). Fabrication of continuous woven E-glass fiber composite using vat photopolymerization additive manufacturing process. *Rapid Prototyping Journal*.

[40] Yilmaz, Y., Ozgul, F., & Agir, I. (2023). An experimental study on low velocity impact characteristics of glass fiber reinforced epoxy nanocomposites. *Sādhanā*, *48*(1), 29.

[41] Lan, K., Wang, H., & Wang, C. (2023). Delamination Behavior of CFRP Laminated Plates under the Combination of Tensile Preloading and Impact Loading. *Materials*, *16*(19), 6595.

[42] Ding, Y., Liu, J., Hall, Z. E., Brooks, R. A., Liu, H., Kinloch, A. J., & Dear, J. P. (2023). Damage and energy absorption behaviour of composite laminates under impact loading using different impactor geometries. *Composite Structures*, 117259.

[43] Barhoumi, H., Bhouri, N., Feki, I., Baffoun, A., Hamdaoui, M., & Ben Abdessalem, S. (2023). Review of ballistic protection materials: Properties and performances. *Journal of Reinforced Plastics and Composites*, *42*(13-14), 685-699.

[44] Palta, E., Fang, H., & Weggel, D. C. (2023). A Numerical Study of the Effects of Projectile Properties on the Impact Behavior of Multi-ply Flexible Fabrics. *Applied Composite Materials*, 1-23.

[45] Yilmaz, M., Ekrem, M., & Avci, A. (2024). Impact resistance of composite to aluminum single lap joints reinforced with graphene doped nylon 6.6 nanofibers. *International Journal of Adhesion and Adhesives*, *128*, 103565.

[46] Păduraru, I., Ojoc, G. G., Păduraru-graur, I., Petrescu, H., & Deleanu, L. (2023). Analyzing Impact Behaviour of Glass Fiber Epoxy Composites for Higher Safety Systems. In *International Conference Knowledge-Based Organization* (Vol. 29, No. 3, pp. 56-64).

[47] Ramesh, S., & Punithamoorthy, K. (2023). Synthesis and characterization of ternary nanocomposites of TiO2/rGO/CdS as an efficient catalyst for photo- degradation of methyl orange. Journal of the Chinese Chemical Society, 70(1), 24-31.

[48] Al Sarraf, A. A. M., Saleh, R. O., Mahmoud, M. Z., Wadday, A. K., & Abed Jawad, M. (2023). Magnetic Nanoparticles Modified With di (Pyridin-2-yl) Amine Ligand Supported Copper Complex: A Novel and Efficient Magnetically Reusable Catalyst for A3 Coupling and CS Cross-Coupling Reactions. *Polycyclic Aromatic Compounds*, *43*(5), 4407-4425.

[49] Moshayedi, H. R., Rabiee, M., & Rabiee, N. (2020). Graphene oxide/polyaniline-based multi nano sensor for simultaneous detection of carbon dioxide, methane, ethanol and ammonia gases. Iranian Journal of Chemistry and Chemical Engineering (IJCCE), 39(3), 93-105.

[50] Yousefi, N., Pazouki, M., Alikhani Hesari, F., & Alizadeh, M. (2016). Statistical evaluation of the pertinent parameters in bio-synthesis of ag/mwf-cnt composites using plackett-burman design and response surface methodology. Iranian Journal of Chemistry and Chemical Engineering (IJCCE), 35(2), 51-62.

[51] Azin, Z., & Pourghobadi, Z. (2021). Electrochemical sensor based on nanocomposite of multi-walled carbon nano-tubes (MWCNTs)/TiO2/carbon ionic liquid electrode analysis of acetaminophen in pharmaceutical formulations. *Iranian Journal of Chemistry and Chemical Engineering*, *40*(4), 1030-1041.

[52] Mallikarjuna, K., Narasimha, G., Dillip, G. R., Praveen, B., Shreedhar, B., Lakshmi, C. S., ... & Raju, B. D. P. (2011). Digest journal of nanomaterials and biostructures. Green synthesis of silver nanoparticles using Occimum leaf extract and their Characterization, 6(1), 181-186.

[53] Ramesh, S., & Punithamoorthy, K. (2019). Synthesis, characterization and gas permeability properties of a novel nanocomposite based on poly (ethylene-co-vinyl acetate)/polyurethane acrylate/clay. Journal of Materials Research and Technology, 8(5), 4173-4181.

[54] Ramesh, S., Kamalarajan, P., & Punithamoorthy, K. (2022). Effect of clay modifier on the structure and transport properties in Polyurethane/Clay Nanocomposites as barrier materials. Iran. J. Chem. Chem. Eng.(IJCCE).